AIP | Physics of Plasmas

The effect of trapped particles on the linear stability of long wavelength resistive modes

R. Fitzpatrick

Citation: Physics of Fluids B: Plasma Physics (1989-1993) **2**, 2636 (1990); doi: 10.1063/1.859387
View online: http://dx.doi.org/10.1063/1.859387
View Table of Contents: http://scitation.aip.org/content/aip/journal/pofb/2/11?ver=pdfcov
Published by the AIP Publishing

Articles you may be interested in
The effect of an anisotropic pressure of thermal particles on resistive wall mode stability
Phys. Plasmas **21**, 112505 (2014); 10.1063/1.4901568

Kinetic effects of trapped energetic particles on stability of external kink modes with a resistive wall
Phys. Plasmas **19**, 032507 (2012); 10.1063/1.3692185

Stabilization of the resistive wall mode instability by trapped energetic particles
Phys. Plasmas **18**, 032513 (2011); 10.1063/1.3569854

Stability of long wavelength modes in tokamaks
Phys. Fluids B **3**, 2061 (1991); 10.1063/1.859672

Effects of collisions on the trapped particle mode in a linear machine
Phys. Fluids **31**, 2695 (1988); 10.1063/1.866548

This article is copyrighted as indicated in the article. Reuse of AIP content is subject to the terms at: http://scitationnew.aip.org/termsconditions. Downloaded to IP: 128.62.18.33 On: Thu, 12 Mar 2015 15:56:36

The effect of trapped particles on the linear stability of long wavelength resistive modes

R. Fitzpatrick
Culham Laboratory (EURATOM/UKAEA Fusion Association), Abingdon, OX14 3DB, England

(Received 26 October 1989; accepted 25 May 1990)

The set of semicollisional layer equations derived by Fitzpatrick [Phys. Fluids B **1**, 2381 (1989)] is used to investigate the effect of trapped particles on the linear stability of long wavelength resistive modes in a large-aspect-ratio tokamak. At $O(1)$ shear, destabilization by trapped particles is found to significantly modify previous cylindrical results for the drift-tearing mode. At low shear, a fairly weak trapped particle-driven interchange (g mode) instability is found, in addition to the usual drift-tearing mode instability, which, in this limit, is virtually unaffected by trapped particles.

I. INTRODUCTION

Long wavelength resistive modes are generally thought to play an important role in determining both global stability and transport in tokamaks. Of particular interest are the $m = 1$ instability, which is associated with "sawtooth" collapses in the plasma core, and the $m = 2$ instability, which is intimately connected with major disruptions. A basic understanding of the stability of these modes is clearly desirable.

As is well known, the determination of the stability of a resistive mode can be reduced to the problem of asymptotically matching a resistive eigenfunction, confined to a thin layer centered on the mode rational surface, to an "outer" ideal magnetohydrodynamic (MHD) eigenfunction that satisfies appropriate boundary conditions at the magnetic axis and the edge of the plasma. In general, the "outer" solution has a logarithmic discontinuity, characterized by a parameter Δ', at the mode rational surface. The matching is performed by setting Δ' equal to a second parameter Δ, which can be expressed in terms of the ratio of the coefficients of the two powerlaw asymptotic forms of the resistive layer solution. This paper is only concerned with the details of the resistive layer (in other words, with the evaluation of Δ). The "outer" solution (and, hence, Δ') can be calculated completely independently (cf. Ref. 1).

Previous linear layer calculations in slab geometry[2,3] have indicated that drift-tearing modes in the so-called "semicollisional" regime (the most appropriate collisionality regime for low mode numbers) are strongly stabilized by electron temperature gradient effects. Other layer calculations[4] have shown that this stabilization extends into the nonlinear regime, but is overcome by parallel thermal conductivity once the island width exceeds some fairly modest value. At present, theory would seem to indicate that semicollisional drift-tearing modes are always linearly stable (at least for $m > 1$), since the critical Δ' that must be exceeded before such modes can become unstable ($\Delta'_c \sim \rho_i^{-1}$) is generally far larger than that which any realistic equilibrium could supply. This conclusion, however, does not take into account the effect of trapped particles. Since it is known[5,6] that, in the linear regime, trapped particles destabilize high and intermediate mode number drift-tearing modes, it would seem reasonable to expect that a similar phenomenon may occur for low mode numbers. Furthermore, a recent study[7] of resistive instabilities in toroidal geometry (neglecting diamagnetic and temperature gradient effects) has shown that trapped particles are a significant destabilizing mechanism in the nonlinear regime, provided that the island size is relatively small. It would seem probable, therefore, that in the linear regime, and also in the nonlinear regime at small island size, there is a competition between the stabilizing effect of the electron temperature gradient and the destabilizing effect of trapped particles. It is not at all clear *a priori* which effect will be dominant. An investigation into trapped particle destabilization of low mode number resistive instabilities would thus appear to be of some interest. This paper is restricted to a discussion of linear theory, which is presented as a first step in the elucidation of some of the points discussed above. Although it is well established[8–11] that at relatively large island size diamagnetic and kinetic effects are not particularly important, there is no reason to suppose that this is the case for the small islands associated with the onset of instability in a mode. For this reason, one can be reasonably optimistic that linear results will be carried over at least a little way into the nonlinear regime. It is interesting to note that while the electron temperature gradient stabilization of modes attenuates fairly rapidly as the island width exceeds the semicollisional layer width, it is unlikely that the trapped particle destabilization behaves in a similar manner, so one can be fairly certain that a mode which is linearly unstable will also be nonlinearly unstable (at least initially).

Hahm[12] has recently derived a linear dispersion relation from a set of collisional neoclassical fluid equations. It is demonstrated that the combined effects of the perturbed bootstrap current and neoclassical flow damping strongly suppress the drift-tearing mode, its place being taken by a fairly virulent neoclassical resistive interchange (g mode) instability. It is obviously of some interest to ascertain whether or not such novel behavior also takes place in the semicollisional regime.

The work presented in this paper is, in many ways, similar to that of Callen *et al.*[13] The major difference is that

This article is copyrighted as indicated in the article. Reuse of AIP content is subject to the terms at: http://scitationnew.aip.org/termsconditions. Downloaded to IP: 128.62.18.33 On: Thu, 12 Mar 2015 15:56:36

Callen *et al.* were unable to take semicollisional effects into account because they restricted themselves to $T_e = \text{const}$. In fact, it turns out that the stability properties of both tearing modes and neoclassical interchange modes are profoundly affected by semicollisional effects.

II. THE LAYER EQUATIONS

The starting point of this investigation is the full set of coupled layer equations presented in Ref. 14. These equations, which describe a resonant mode in toroidal geometry, were derived from the gyrokinetic equation using a model collision operator. The following set of assumptions was made.

(i) The mode is "linear," i.e., the island width is small in comparison to the layer width.

(ii) The underlying equilibrium is that of a low-beta, large-aspect-ratio tokamak.

(iii) The plasma is "hot," i.e., the ions and electrons both lie in the banana regime and the layer physics is either "semicollisional" or weakly "collisional."

(iv) The ions and electrons are "fluid-like," i.e., the ion and electron collision frequencies are significantly larger than the mode frequency.

(v) The ion Larmor radius is "small," i.e., it is significantly less than the layer width.

(vi) The following hierarchies of electron and ion frequencies are valid:

$$\omega_{\rm tr} \gg \nu_e, \quad \mathbf{k}_r\cdot\mathbf{v}_d \gg k_\parallel v_\parallel \gg \omega, \quad \mathbf{k}_\theta\cdot\mathbf{v}_d$$

and

$$(\omega_{\rm tr})_i \gg \nu_i, \quad (\mathbf{k}_r\cdot\mathbf{v}_d)_i \gg \omega \gg (k_\parallel v_\parallel)_i, \quad (\mathbf{k}_\theta\cdot\mathbf{v}_d)_i \gg \omega(\rho_i/|\delta_e|)^2.$$

Here, $\omega_{\rm tr}$ is the electron transit frequency, ν_e is the electron collision frequency, $\mathbf{k}_r\cdot\mathbf{v}_d$ is the electron magnetic drift frequency across the layer, $k_\parallel v_\parallel$ is the electron Doppler frequency due to thermal streaming along field lines, ω is the mode frequency, and $\mathbf{k}_\theta\cdot\mathbf{v}_d$ is the electron magnetic drift frequency along the layer. Similar frequencies are also defined for the ions (denoted by the subscript i). The quantities $\mathbf{k}$, ρ_i, and $|\delta_e|$ are the wave vector, the ion Larmor radius, and the layer width, respectively.

Assumption (i) is the hardest to justify since a simple-minded calculation of the island size likely to be induced by stray error fields generally gives an answer that is larger than the semicollisional layer width. Forced reconnection is, however, a far more complex problem than conventional reconnection, because the forcing frequency is highly unlikely to be one of the natural mode frequencies owing to the combined effects of bulk toroidal rotation and diamagnetism. When a reconnecting mode is excited at a frequency other than its natural frequency strong flows are induced around the magnetic island which tend to be highly stabilizing. It can easily be shown (by a calculation along the lines of Hahm and Kulsrud[15]) that in the linear regime the amount of reconnection likely to be induced by error fields is substantially reduced by the abovementioned effect. Recent calculations[16] have indicated that a similar phenomenon occurs in the nonlinear regime at small island size. For these reasons, one can be fairly optimistic that, in practice, linear theory is not invalidated by stray error fields.

Assumption (ii) is standard for a tokamak ordering. Incidentally, the assumption of low beta justifies the neglect of poloidal currents.

Assumption (iii) is reasonable in modern high-temperature (i.e., $\geqslant 1$ keV) tokamaks.

As is discussed in Ref. 14, assumption (iv) can probably only be justified for low mode number (i.e., $m \leqslant 2$).

Assumption (v) is questionable for linear modes unless the shear at the rational surface is small (there is some evidence that this is, in fact, the case for $m = 1$ modes[17]). Note that there are strong indications that the stability properties of semicollisional modes are not strongly influenced by finite ion Larmor radius effects (e.g., note the marked similarity between the semicollisional stability criterion calculated in Ref. 2, for the case where the ion Larmor radius is much less than the layer width, and the criterion calculated in Ref. 3 for the opposite case).

The hierarchies of electron and ion frequencies in (vi) are actually chosen to facilitate the derivation of the neoclassical layer equations. However, as is discussed in Ref. 14, they are quite reasonable for low mode number instabilities in modern tokamaks. In fact, a recent study by the author of data from typical Ohmic JET[18] discharges has shown that these hierarchies are particularly appropriate for $m = 1$ modes when the shear at the rational surface is small.

The neoclassical layer equations can be written in the following normalized form:

$$\begin{aligned}0 = {} & \hat\omega\,\delta\nu + \bar\sigma_\parallel\{s^2(\delta\nu + \lambda_\alpha^\parallel\delta\tau) + [\hat\omega - (1+\lambda_\alpha^\parallel\eta)](A - s\psi)\} - \kappa_B[\hat\omega + \tau(1+\bar\alpha_i\eta_i)]\frac{d\psi}{ds} + (\zeta\epsilon^{1/2})\alpha_n^B\kappa_B\frac{d}{ds}\{s(\delta\nu \\ & + \lambda_\alpha^B\delta\tau) + [(1+\lambda_\alpha^B\eta) + \tau(1+\bar\alpha_i\eta_i)]\psi\} - (\zeta\epsilon^{1/2})\alpha_n^P\kappa_B\frac{1}{s}\frac{d}{ds}\{s^2(\delta\nu + \lambda_\alpha^P\delta\tau) + [\hat\omega - (1+\lambda_\alpha^P\eta)](A - s\psi)\} \\ & + (\zeta\epsilon^{1/2})\alpha_n^D\kappa_B^2\frac{1}{s}\frac{d^2}{ds^2}\{s(\delta\nu + \lambda_\alpha^D\delta\tau) + [(1+\lambda_\alpha^D\eta) + \tau(1+\bar\alpha_i\eta_i)]\psi\},\end{aligned} \qquad (1)$$

This article is copyrighted as indicated in the article. Reuse of AIP content is subject to the terms at: http://scitationnew.aip.org/termsconditions. Downloaded to IP: 128.62.18.33 On: Thu, 12 Mar 2015 15:56:36

$$0=\frac{3}{2}\,\hat{\omega}\,(\delta\nu+\delta\tau)+\overline{\kappa}_{\parallel}\{s^2(\delta\nu+\lambda_\beta^{\parallel}\delta\tau)+[\,\hat{\omega}-(1+\lambda_\beta^{\parallel}\eta)\,](A-s\psi)\}-\frac{5}{2}\kappa_B[\,\hat{\omega}+\tau(1+\overline{\alpha}_i\eta)\,]\frac{d\psi}{ds}$$

$$+(\zeta\epsilon^{1/2})\beta_n^B\kappa_B\frac{d}{ds}\{s(\delta\nu+\lambda_\beta^B\delta\tau)+[\,(1+\lambda_\beta^B\eta)+\tau(1+\overline{\alpha}_i\eta_i)\,]\psi\}-(\zeta\epsilon^{1/2})\beta_n^P\kappa_B\frac{1}{s}\frac{d}{ds}\{s^2(\delta\nu+\lambda_\beta^P\delta\tau)$$

$$+[\,\hat{\omega}-(1+\lambda_\beta^P\eta)\,](A-s\psi)\}+(\zeta\epsilon^{1/2})\beta_n^D\kappa_B^2\frac{1}{s}\frac{d^2}{ds^2}\{s(\delta\nu+\lambda_\beta^D\delta\tau)+[\,(1+\lambda_\beta^D\eta)+\tau(1+\overline{\eta}_i\eta_i)\,]\psi\}, \tag{2}$$

$$0=\hat{\beta}^{-1}s\frac{d^2A}{ds^2}+\kappa_B\frac{d}{ds}\{s^2(\delta\nu+\delta\tau)-[\,(1+\eta)+\tau(1+\eta_i)\,](A-s\psi)\}-iC_{\rm eff}^{-1}\hat{\omega}\,[\,\hat{\omega}+\tau(1+\overline{\alpha}_i\eta_i)\,]\frac{d^2\psi}{ds^2}, \tag{3}$$

$$0=\hat{\beta}^{-1}\frac{d^2A}{ds^2}+\overline{\sigma}_{\parallel}\{s^2(\delta\nu+\lambda_\alpha^{\parallel}\delta\tau)+[\,\hat{\omega}-(1+\lambda_\alpha^{\parallel}\eta)\,](A-s\psi)\}+(\zeta\epsilon^{1/2})\alpha_n^B\kappa_B\frac{d}{ds}\{s(\delta\nu+\lambda_\alpha^B\delta\tau)+[\,(1+\lambda_\alpha^B\eta)$$

$$+\tau(1+\overline{\alpha}_i\eta_i)\,]\psi\}. \tag{4}$$

Here,

$$\delta_e^2=-i\left(\frac{2\omega_*\nu_e l_s^2}{v_{\rm th}^2k_\theta^2}\right),\quad s=\frac{x}{\delta_e},\quad \hat{\omega}=\frac{\omega}{\omega_*},\quad \psi=-\left(\frac{ck_\theta\delta_e}{\omega l_s}\right)\Phi,\quad \delta\nu=i\left(\frac{m_e c v_e}{(-e)k_\parallel}\right)\frac{\delta n}{n},\quad \delta\tau\left(\frac{m_e c v_e}{(-e)k_\parallel}\right)\frac{\delta T}{T}, \tag{5}$$

where A is the perturbed magnetic vector potential, Φ is the perturbed electrostatic potential, δn and δT are the semicollisional contributions to the perturbed electron density and temperature, $v_{\rm th}=2T_e/m_e$ is the electron thermal velocity, x the radial distance from the center of the layer, ϵ the inverse aspect ratio, $\omega_*=-ck_\theta T_e/ZeBl_n$ is the electron diamagnetic frequency, $l_s=Rq^2/rq'$ is the magnetic shear length, and $l_n=-[d(\ln n_e)/dr]^{-1}$ is the density scale length. (N.B. All equilibrium quantities are evaluated at the mode rational surface.) The constants ζ, $\overline{\sigma}_\parallel$, $\overline{\kappa}_\parallel$, $\lambda_n^\parallel$, α_n^B, β_n^B, etc., are all $O(1)$ electron transport parameters that are defined and evaluated in Ref. 14. (Note, however, that in this paper α_n^D, α_T^D, β_n^D, and β_T^D are redefined to be twice the equivalent parameters in Ref. 14 in order to eliminate some stray factors of 2 in the layer equations.)

The first two equations ensure electron number and energy conservation, and include the effects of neoclassical transport as well as the neoclassical modification to the Spitzer parallel electrical and thermal conductivities. The third equation describes the evolution of the flow vorticity, and takes into account both neoclassical poloidal flow damping and ion polarization drift. The last equation is Ohm's law, including the effect of the bootstrap current. Since the above layer equations take into account the effects of semicollisional temperature gradient stabilization, trapped particle destabilization, and neoclassical flow damping, they are ideally suited to the investigation at hand. Note that curvature has been neglected, since it is formally $O(\epsilon^2)$ whereas the other neoclassical effects are $O(\epsilon^{1/2})$. Note also that the equations have been generalized to take account of the following two new effects.

(i) The effect of impurity ions. [N.B. All impurities are assumed to lie in the banana regime and have "small" Larmor radii—this rules out "heavy" impurities (e.g., Fe), "fast" ions, and alpha particles.] In the presence of impurities, the electron transport parameters ($\alpha_n^\parallel$, etc.) are still evaluated in accordance with Tables I–IV of Ref. 14, except that Z is now replaced by

$$Z_{\rm eff}=\sum_{\substack{j\\ \text{(ion species)}}}\frac{Z_j^2 n_j}{n_e}. \tag{6}$$

(ii) The effect of finite ion temperature. The analysis of this effect introduces the parameter

$$\tau=Z^{-1}(T_i/T_e), \tag{7}$$

as well as the ion transport parameter

$$\overline{\alpha}_i=\alpha_i(1-A_i\zeta\epsilon^{1/2}). \tag{8}$$

Expressions for α_i and A_i are given in Ref. 14. The inclusion of finite ion temperature effects is necessary for the correct evaluation of the growth rates of low-frequency modes.

The layer equations (1)–(4) are written in terms of the following eight fundamental parameters.

(1) $Z_{\rm eff}$: the effective ion charge number due to the presence of impurity ions.

(2) $C_{\rm eff}^{-1}\equiv Z^{-1}\,\omega^* m_{i\,{\rm eff}}l_n^2/\nu_e m_e l_s^2$: a measure of the effective collisionality of the layer. Here, $m_{i\,{\rm eff}}=m_i(1+B^2/B_\theta^2)$ is the effective ion mass. The ions act as if they have this greatly enhanced mass because of the effect of neoclassical flow damping. When $C_{\rm eff}\ll 1$ the layer is "semicollisional"; when $C_{\rm eff}\gg 1$ the layer is "collisional."

(3) $\kappa_B\equiv Bl_n/B_\theta l_s=-d(\ln q)/d(\ln n_e)$: a measure of the magnetic shear at the rational surface. When $\kappa_B\sim O(1)$ the shear is $O(1)$.

(4) $\hat{\beta}\equiv 4\pi(nT)_e/\kappa_B^2B_\theta^2$: a strongly shear-dependent measure of the local electron pressure.

(5) $\eta\equiv d(\ln T_e)/d(\ln n_e)$.

(6) $\eta_i\equiv d(\ln T_i)/d(\ln n_i)$.

This article is copyrighted as indicated in the article. Reuse of AIP content is subject to the terms at: http://scitationnew.aip.org/termsconditions. Downloaded to IP: 128.62.18.33 On: Thu, 12 Mar 2015 15:56:36

(7) $\zeta\epsilon^{1/2}$: a measure of the fraction of trapped particles.

(8) $\tau \equiv Z^{-1}T_i/T_e$: minus the ratio of the ion diamagnetic frequency to the electron diamagnetic frequency.

Of these eight parameters $Z_{\rm eff}, \eta_i$, and τ are relatively unimportant. The parameters $C_{(\rm eff)}$ and $\hat{\beta}$ were first introduced into tearing mode theory by Drake *et al.*[2]

As explained in Ref. 14, the layer solution is matched to the "outer" ideal MHD solution via an "intermediate" layer, for which $(k_\parallel v_\parallel)_i \sim \omega$. It can be shown that the boundary conditions applicable to Eqs. (1)–(4) are

$$A \to a_-\left[1 + O\left(\frac{1}{s^2}\right)\right] + a_+ s\left[1 + O\left(\frac{1}{s^2}\right)\right],$$

$$\psi \to a_-\left(\frac{\hat{\omega}(\hat{\omega}-1)}{\hat{\omega}(\hat{\omega}-1)+\kappa_B Q_i^\parallel}\right)\frac{1}{s}\left[1 + O\left(\frac{1}{s^2}\right)\right] + a_+\left[1 + O\left(\frac{1}{s^2}\right)\right], \tag{9}$$

as $s \to e^{i\pi/4}\infty$, where

$$\frac{a_+}{a_-} = \left[\frac{\hat{\omega}(\hat{\omega}-1) + \kappa_B Q_i^\perp + (\kappa_B^2\hat{\beta})Q_i^\parallel Q_i^\perp}{\hat{\omega}(\hat{\omega}-1)+\kappa_B Q_i^\parallel}\right] \times \frac{1}{2} e^{-i\pi/4} C_{\rm eff}^{1/2} \Delta \rho_{s\,\rm eff}. \tag{10}$$

Here,

$$\rho_{s\,\rm eff} = (T_e m_{i\,\rm eff}/Z)^{1/2}(c/eB), \tag{11}$$

and

$$Q_i^\parallel = \hat{\omega} + \tau(1 + \bar{\alpha}_i \eta_i), \quad Q_i^\perp = \hat{\omega} + \tau(1 + \eta_i). \tag{12}$$

The frequency-dependent quantity $\Delta(\omega)$ completely determines the stability properties of the layer.

III. ANALYSIS

If all $\zeta\epsilon^{1/2}$ terms are neglected Eqs. (1)–(4) reduce to a set of coupled fourth-order complex equations, which can readily be solved by shooting in real space. The asymptotic forms at large $|s|$ consist of the two power-law solutions required by the boundary conditions (9), plus a damped exponential solution and a growing exponential solution. This last solution is unphysical and must, therefore, be suppressed. Unfortunately, as soon as the $\zeta\epsilon^{1/2}$ terms are reinstated the system becomes eighth order in complex variables and acquires two more unphysical asymptotic forms at large $|s|$. The simultaneous elimination of three violently growing solutions, plus the retention of two power-law solutions, at large $|s|$ is a fairly formidable computing problem; however, the situation becomes significantly less complicated in Fourier transform space. In fact, in transform space the system is at most fifth order in complex variables. Furthermore, in marked contrast with the situation in real space, there are no violently exponentiating solutions present in the region of transform space where the asymptotic matching with the "outer" solution is performed.

Let

$$\bar{f}(p) = \int f(s) e^{ips}\, ds; \tag{13}$$

then the layer equations (1)–(4) Fourier transform to the following:

$$0 = c_2\hat{\omega} Q_0\phi_1 - \frac{d^2}{dp^2}[Q_\alpha^\parallel(\phi_1+\phi_A-\phi_\psi) + P_\alpha^\parallel\phi_2] + c_2 Q_i^\parallel\frac{d}{dp}(p\phi_\psi) - c_1c_2\frac{d}{dp}p(Q_\alpha^B\phi_1 + P_\alpha^B\phi_2 + R_\alpha^B\phi_\psi) + c_1c_2p\frac{d}{dp}[Q_\alpha^P(\phi_1+\phi_A-\phi_\psi) + P_\alpha^P\phi_2] - c_1c_2^2p^2(Q_\alpha^D\phi_1 + P_\alpha^D\phi_2 + R_\alpha^D\phi_\psi), \tag{14}$$

$$0 = \frac{3}{2}\hat{\omega}Q_1\phi_1 + \frac{3}{2}\hat{\omega}P_1\phi_2 - \frac{d^2}{dp^2}[Q_\beta^\parallel(\phi_1+\phi_A-\phi_\psi) + P_\beta^\parallel\phi_2] + \frac{5}{2}c_2Q_i^\parallel\frac{d}{dp}(p\phi_\psi) - c_1c_2\frac{d}{dp}p(Q_\beta^B\phi_1 + P_\beta^B\phi_2 + R_\beta^B\phi_\psi) + c_1c_2p\frac{d}{dp}[Q_\beta^P(\phi_1+\phi_A-\phi_\psi) + P_\beta^P\phi_2] - c_1c_2^2p^2(Q_\beta^D\phi_1 + P_\beta^D\phi_2 + R_\beta^D\phi_\psi), \tag{15}$$

$$0 = \frac{d}{dp}(\phi_1+\phi_A-\phi_\psi) + \hat{\sigma}_{E\psi}p\phi_\psi + \hat{\sigma}_{E1}p\phi_1 + \hat{\sigma}_{E2}p\phi_2 + \hat{\sigma}_E\frac{d\phi_2}{dp} - \hat{\sigma}_{Ei}\frac{d\phi_\psi}{dp}, \tag{16}$$

where

$$\phi_A = \overline{A/s}, \quad \phi_\psi = \bar{\psi},$$

$$\phi_1 = \frac{(\overline{s\delta v})}{\hat{\omega}-1}, \quad -\eta\phi_2 = \frac{[\eta(\overline{s\delta v}) + (\hat{\omega}-1)(\overline{s\delta\tau})]}{\hat{\omega}-1}, \tag{17}$$

and

$$Q_0 = (\hat{\omega}-1)/\kappa_B,$$

$$Q_1 = (\hat{\omega}-1) - \eta,$$

$$P_1 = -\eta,$$

This article is copyrighted as indicated in the article. Reuse of AIP content is subject to the terms at: http://scitationnew.aip.org/termsconditions. Downloaded to IP: 128.62.18.33 On: Thu, 12 Mar 2015 15:56:36

$$Q^{\parallel}_{\alpha,\beta}=\{\alpha,\beta\}^{\parallel}_{n}[1-(1+\{A,B\}_{n})\zeta\epsilon^{1/2}](\hat{\omega}-1)$$
$$-\{\alpha,\beta\}^{\parallel}_{T}[1-(1+\{A,B\}_{T})\zeta\epsilon^{1/2}]\eta,$$
$$P^{\parallel}_{\alpha,\beta}=-\{\alpha,\beta\}^{\parallel}_{T}[1-(1+\{A,B\}_{T})\zeta\epsilon^{1/2}]\eta,$$
$$Q^{B,P,D}_{\alpha,\beta}=\{\alpha,\beta\}^{B,P,D}_{n}(\hat{\omega}-1)-\{\alpha,\beta\}^{B,P,D}_{T}\eta,$$
$$P^{B,P,D}_{\alpha,\beta}=-\{\alpha,\beta\}^{B,P,D}_{T}\eta,$$
$$R^{B,D}_{\alpha,\beta}=\{\alpha,\beta\}^{B,D}_{n}+\{\alpha,\beta\}^{B,D}_{T}\eta+\{\alpha,\beta\}^{B,D}_{n}\tau(1+\bar{\alpha}_{i}\eta_{i}),$$
$$R_{i}=Q^{\perp}_{i}-Q^{\parallel}_{i}=\tau(1-\bar{\alpha}_{i})\eta_{i},$$
$$c_1=\zeta\epsilon^{1/2},$$
$$c_2=\kappa_B, \tag{18}$$
$$c_3=iC_{\rm eff}^{-1}/\kappa_B,$$
$$c_4=\hat{\beta},$$
with
$$\hat{\sigma}_{E\psi}=\left(\frac{(Q^{\parallel}_{i}+c_1c_2c_4Q^{\perp}_{i}R^{B}_{\alpha})+(c_3\hat{\omega}Q^{\parallel}_{i}-c_1c_2R^{D}_{\alpha})p^2}{c_4Q^{\perp}_{i}Q^{\parallel}_{\alpha}-(Q_1-c_1Q^{P}_{\alpha})p^2}\right),$$
$$\hat{\sigma}_{E1}=\left(\frac{(\hat{\omega}Q_0+c_1c_2c_4Q^{\perp}_{i}Q^{B}_{\alpha})-c_1c_2Q^{D}_{\alpha}p^2}{c_4Q^{\perp}_{i}Q^{\parallel}_{\alpha}-(Q_1-c_1Q^{P}_{\alpha})p^2}\right),$$
$$\hat{\sigma}_{E2}=\left(\frac{c_1c_2c_4Q^{\perp}_{i}P^{B}_{\alpha}-c_1c_2P^{D}_{\alpha}p^2}{c_4Q^{\perp}_{i}Q^{\parallel}_{\alpha}-(Q_1-c_1Q^{P}_{\alpha})p^2}\right),$$
$$\hat{\sigma}_{E}=\left(\frac{c_4Q^{\perp}_{i}P^{\parallel}_{\alpha}-(P_1-c_1P^{P}_{\alpha})p^2}{c_4Q^{\perp}_{i}Q^{\parallel}_{\alpha}-(Q_1-c_1Q^{P}_{\alpha})p^2}\right), \tag{19}$$
$$\hat{\sigma}_{Ei}=\left(\frac{R_i p^2}{c_4Q^{\perp}_{i}Q^{\parallel}_{\alpha}-(Q_1-c_1Q^{P}_{\alpha})p^2}\right).$$

The quantity ϕ_A can readily be eliminated between Eqs. (14)–(16). The resulting system of equations is, in general, fifth order in complex variables. However, for the special case $\eta_i=0$ the system reduces to fourth order. Note that the order of the transformed equations is not affected when $\zeta\epsilon^{1/2}\to 0$. The fact that the order of the system increases when $\eta_i\neq 0$ probably indicates the presence of a mode specifically associated with η_i. Since such modes are not of primary interest in this paper, only the simplest case $\eta_i=0$ will be considered from now on.

The fourth-order system under consideration has three physically acceptable small $|p|$ asymptotic expansions. These can be written schematically:

$$\phi_\psi\sim(b_{(-1)}/p)[1+O(p^2)]+b_{(0)}[1+O(p^2)]$$
$$+b_{(1)}p[1+O(p^2)]. \tag{20}$$

The fourth asymptotic expansion is unacceptable because its inverse Fourier transform is not a large $|s|$ solution of the real-space layer equations. The real-space boundary conditions (9) and (10) Fourier transform to

$$\frac{b_{(-1)}}{b_{(0)}}=\frac{2}{\pi}\left(\frac{\hat{\omega}Q_0+Q_i+c_2c_4Q_iQ_i}{\hat{\omega}Q_0+Q_i}\right)\times\frac{1}{2}e^{-i\pi/4}C_{\rm eff}^{1/2}\Delta\rho_{s\,{\rm eff}}, \tag{21}$$

where

$$Q_i=\hat{\omega}+\tau. \tag{22}$$

At large $|p|$, the system under consideration has four exponential asymptotic solutions of the form $\exp(p^2/2k_{1\to 4})$. Two of these grow along the Fourier transformed radial axis, the other two are damped—by convention the solutions associated with k_1 and k_2 are the growing ones. Note that in the limit as $\zeta\epsilon^{1/2}\to 0$, the form of these large $|p|$ asymptotic solutions changes to $\exp(p/l_{1\to 4})$.

A numerical dispersion relation can be obtained from Eqs. (14)–(16) by following the procedure set out below.

(1) Choose a value for $\hat{\omega}$.

(2) Choose a convenient axis in complex p space (the $\bar{y}$ axis, say) that passes through the origin and lies in the region of p space where $\exp(p^2/2k_1)$ and $\exp(p^2/2k_2)$ are both growing.

(3) Numerically integrate the system along the $\bar{y}$ axis from very small $\bar{y}$ to large positive $\bar{y}$. Since the system is undetermined to an arbitrary multiplicative constant there are only two free parameters at small $\bar{y}$—namely, $b_{(-1)}/b_{(0)}$ and $b_{(1)}/b_{(0)}$. In general, after launching three test solutions from small $\bar{y}$, two basis solutions can be constructed which have zero component of the most virulent exponentiating asymptotic form at large $\bar{y}$.

(4) By launching the two basis solutions from small $\bar{y}$ along the $\bar{y}$ axis, infer the linear combination of these which has zero component of the remaining exponentiating asymptotic form at large $\bar{y}$. By this stage the free parameters $b_{(-1)}/b_{(0)}$ and $b_{(1)}/b_{(0)}$ are fully determined.

(5) Calculate $\Delta(\hat{\omega})$ from $b_{(-1)}/b_{(0)}$, making use of Eq. (21).

(6) Vary $\mathrm{Re}(\hat{\omega})$ until Δ is real. This is necessary because a complex Δ is physically meaningless.

Once steps (1)–(6) have been carried out, Δ and $\mathrm{Re}(\hat{\omega})$ remain as functions of $\mathrm{Im}(\hat{\omega})$.

A computer code has been developed to derive a dispersion relation from Eqs. (14)–(16) in accordance with the plan of action set out above. It is encouraging that this code is found to reproduce the numerical results of Ref. 14, to a high degree of accuracy, when $\zeta\epsilon^{1/2}\to 0.0$, $Z_{\rm eff}=1.0$, and $\tau=0.0$. The new results, for $\zeta\epsilon^{1/2}>0$, are presented in the next section.

IV. RESULTS

The typical behavior at $O(1)$ shear is illustrated in Fig. 1, which shows the critical Δ required for the marginal stability of the drift-tearing mode plotted as a function of the collisionality parameter $C_{\rm eff}$, and parametrized by the fraction of trapped particles $\zeta\epsilon^{1/2}$. Clearly, even the presence of a fairly modest fraction of trapped particles ($\epsilon^{1/2}=0.1$) has such a strong destabilizing effect in the semicollisional regime ($C_{\rm eff}<1$) that electron temperature gradient stabilization of the mode (shown in the $\epsilon^{1/2}=0.0$ curve) is completely overwhelmed. It is apparent that with a realistic fraction of trapped particles and $O(1)$ shear at the rational surface, the drift-tearing mode will be linearly unstable in the semicollisional regime unless Δ falls below

This article is copyrighted as indicated in the article. Reuse of AIP content is subject to the terms at: http://scitationnew.aip.org/termsconditions. Downloaded to IP: 128.62.18.33 On: Thu, 12 Mar 2015 15:56:36

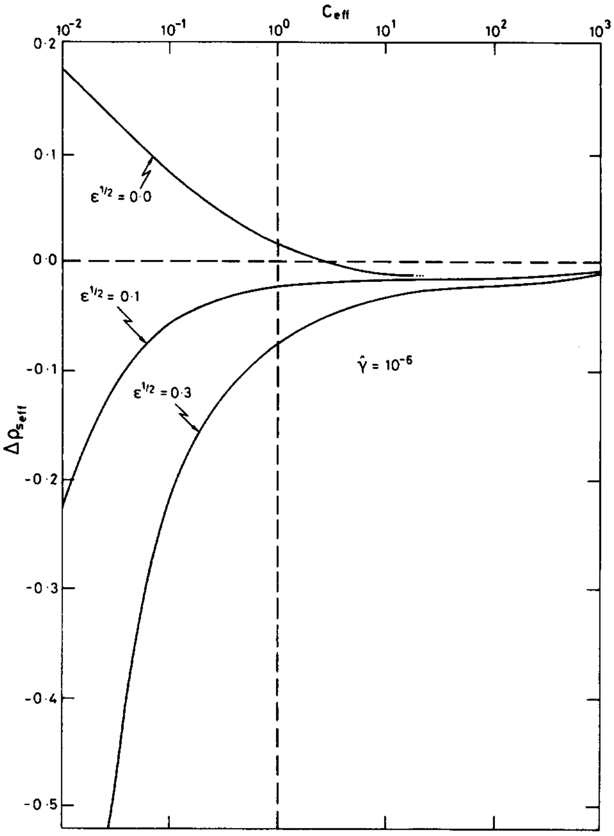

FIG. 1. The critical Δ (scaled by $\rho_{s\,\mathrm{eff}}^{-1}$) required for marginal stability, plotted as a function of the collisionality parameter C_{eff}, for $\kappa_B = 1.0$, $\epsilon^{1/2} = (0.0, 0.1, 0.3)$, $\hat{\beta} = 0.1$, $\eta = 1.0$, $\eta_i = 0.0$, $\tau = 0.1$, and $Z_{\mathrm{eff}} = 1.0$. The mode is unstable if Δ exceeds the critical Δ, and stable otherwise. The quantity $\hat{\gamma}$ is the growth rate normalized with respect to the electron diamagnetic frequency.

some large negative threshold value ($\Delta_c \sim -\rho_i^{-1}$). This is a significant new result since it shows that previous thinking on the stability of low mode number resistive instabilities in the semicollisional regime is incorrect. This result also demonstrates the crucial importance of including toroidicity in linear resistive layer calculations. Presumably, the same is also true of nonlinear calculations when the island size is relatively small.

The typical behavior at small shear is illustrated in Fig. 2, where the critical Δ for marginal stability is again plotted as a function of collisionality. Note that at low shear trapped particles are completely ineffective at destabilizing the drift-tearing mode, and the cylindrical results of Ref. 2 hold to a good approximation. This is yet another example of a situation where small shear at the rational surface can stabilize low mode number tearing modes. Such effects are particularly significant for $m = 1$, since at present it is difficult to account for the fact that equilibria with central q values lying well below unity can apparently be linearly stable to $m = 1$ modes.

Also plotted in Fig. 2 are the marginal stability curves of a new type of mode that only becomes unstable when the shear is small. It is clear from the scaling with $\epsilon^{1/2}$ (two values, $\epsilon^{1/2} = 0.1$ and 0.3, are plotted) that this mode is driven unstable primarily by trapped particles. Not surprisingly, the mode disappears altogether in the limit as $\epsilon^{1/2} \rightarrow 0$. Figure 3 shows how the growth rate of this new mode varies as a function of Δ at constant collisionality. The variation of the drift-tearing mode growth rate is also shown for comparison. Note that the new mode is relatively insensitive to Δ and is most unstable close to $\Delta = 0$, in marked contrast to the tearing mode. The new mode is also found to have a significantly smaller real frequency than the tearing mode. Such properties are characteristic of an interchange (g mode) instability, where the major driving force is internal to the layer (in this case, the perturbed bootstrap current). It is with a fair degree of confidence, then, that this new mode can be identified with the neoclassical interchange mode discussed in Ref. 12. Note that the collisional layer equations used in Ref. 12 are only

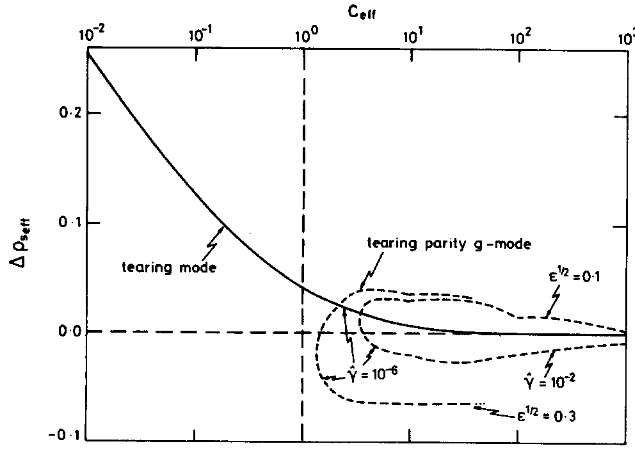

FIG. 2. The critical Δ required for marginal stability, plotted as a function of the collisionality parameter C_{eff}, for $\kappa_B = 0.1$, $\epsilon^{1/2} = (0.1, 0.3)$, $\hat{\beta} = 0.1$, $\eta = 1.0$, $\eta_i = 0.0$, $\tau = 0.1$, and $Z_{\mathrm{eff}} = 1.0$. The solid curve represents the drift-tearing root (the mode is unstable if Δ lies above the curve, and vice versa). The dashed curve represents the g-mode root (this mode is unstable if Δ lies inside the closed curve, and stable otherwise).

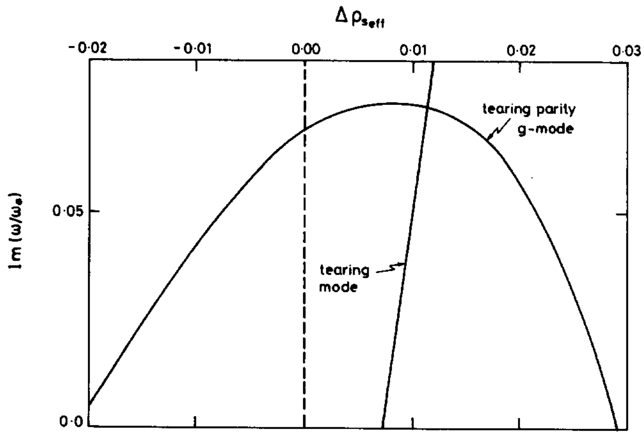

FIG. 3. The growth rates of the drift-tearing and g-mode roots (normalized with respect to the electron diamagnetic frequency) plotted as a function of Δ, for $C_{\mathrm{eff}} = 10.0$, $\kappa_B = 0.1$, $\epsilon^{1/2} = 0.1$, $\hat{\beta} = 0.1$, $\eta = 1.0$, $\eta_i = 0.0$, $\tau = 0.1$, and $Z_{\mathrm{eff}} = 1.0$.

This article is copyrighted as indicated in the article. Reuse of AIP content is subject to the terms at: http://scitationnew.aip.org/termsconditions. Downloaded to IP: 128.62.18.33 On: Thu, 12 Mar 2015 15:56:36

valid (i) if the shear is low, and (ii) if the collisional layer width is much less than the semicollisional layer width (i.e., if $C_{\rm eff}^{1/4} \gg 1$). Unfortunately, for technical reasons the computer code used to derive the data shown in Figs. 1–3 can only operate with $C_{\rm eff} \leqslant 10^3$, which is still not sufficiently collisional for condition (ii) to be well satisfied. A quantitative comparison with the dispersion relation of Hahm is therefore not possible.

Note that there is no sign of a strong suppression of the drift-tearing mode by neoclassical effects in Figs. 2 and 3. The major effect of neoclassical flow damping is to enhance the ion mass by a factor $(1 + B^2/B_\theta^2)$. This enhancement has the effect of decreasing the collisionality of the system, but simultaneously increases the scale length ρ_s—these two effects largely cancel one another out in the determination of the drift-tearing mode growth rate. At low shear, the perturbed bootstrap current appears to have little influence on the tearing mode. Clearly, the suppression of the drift-tearing mode by neoclassical effects at low shear reported by Hahm can only occur at extremely high collisionality. In the range of collisionalities appropriate to low mode number instabilities in a modern tokamak ($10^{-2} < C_{\rm eff} < 10$, say) such behavior is not observed.

It is also clear from Figs. 2 and 3 that the neoclassical interchange mode is fairly placid at realistic collisionalities. This result follows, first, since the mode is only significant close to $\Delta = 0$, second, since it only seems to have a fairly modest growth rate, and third, since it does not extend into the semicollisional regime at all. These results do not seem to bear out the speculation in Ref. 12 that neoclassical interchange modes can dominate drift-tearing modes—at least, not at low mode number.

V. CONCLUSIONS

It is clear that trapped particles can have a profound effect on the linear stability properties of low mode number resistive instabilities. When the shear at the rational surface is $O(1)$, the drift-tearing mode is strongly destabilized by the perturbed bootstrap current in the semicollisional regime. Under normal circumstances, this destabilizing effect dominates the semicollisional electron temperature gradient stabilization of Ref. 2. However, if the shear at the rational surface is small then the effect of the perturbed bootstrap current on the drift-tearing mode becomes negligible, and the stabilizing influence of the electron temperature gradient predominates in the semicollisional regime. The perturbed bootstrap current manifests itself at low shear by destabilizing a resistive interchange mode (presumably the same mode as is discussed in Ref. 12). However, this mode is not particularly strong at realistic collisionalities, and appears to be completely stable in the semicollisional regime. As is demonstrated in Ref. 14, and also discussed briefly in Sec. IV of this paper, neoclassical flow damping only has a fairly weak influence on the stability of low mode number resistive instabilities in realistic collisionality regimes.

Obviously, linear results only have a very limited application to experiments since most modes are already well into their nonlinear phases by the time they have become strong enough to be detected. Linear dispersion relations do have their uses, however; in particular, if they are coupled with an equilibrium evolution code and a toroidal Δ' code (such as the one described in Ref. 1) they can be used to predict the *onset* of instability in a mode. Now, it is well known that toroidicity plays an important part in determining the mode structure external to the layer, and hence in determining Δ' at the rational surface (especially for $m = 1$). What is clear from the results presented in this paper is that toroidicity is just as important when it comes to determining the resistive layer solution.

ACKNOWLEDGMENTS

The author would like to thank J. W. Connor and R. J. Hastie for many helpful comments and discussions. The author also acknowledges the assistance of Dr. David Campbell in obtaining JET discharge data.

[1] J. W. Connor, S. C. Cowley, R. J. Hastie, T. C. Hender, A. Hood, and T. S. Martin, Phys. Fluids **31**, 577 (1988).
[2] J. F. Drake, T. M. Antonsen, A. B. Hassam, and N. T. Gladd, Phys. Fluids **26**, 2509 (1983).
[3] S. C. Cowley, R. M. Kulsrud, and T. S. Hahm, Phys. Fluids **29**, 3230 (1986).
[4] B. D. Scott and A. B. Hassam, Phys. Fluids **30**, 90 (1987).
[5] P. J. Catto and M. N. Rosenbluth, Phys. Fluids **24**, 243 (*1981*).
[6] J. W. Connor, S. C. Cowley, and R. J. Hastie, to appear in Plasma Phys. Controlled Fusion.
[7] R. Carrera, R. D. Hazeltine, and M. Kotschenreuther, Phys. Fluids **29**, 899 (1986).
[8] H. R. Hicks, B. A. Carreras, and J. A. Holmes, Phys. Fluids **27**, 909 (1984).
[9] D. Biskamp, Nucl. Fusion **19**, 777 (1979).
[10] J. F. Drake and Y. C. Lee, Phys. Rev. Lett. **39**, 453 (1977).
[11] B. D. Scott, A. B. Hassam, and J. F. Drake, Phys. Fluids **28**, 275 (1985).
[12] T. S. Hahm, Phys. Fluids **31**, 3709 (1988).
[13] J. D. Callen, W. X. Qu, K. D. Siebert, B. A. Carreras, K. C. Shaing, and D. A. Spong, in *Plasma Physics and Controlled Nuclear Fusion Research 1986* (IAEA, Vienna, 1987), Vol. II, p. 157.
[14] R. Fitzpatrick, Phys. Fluids B **1**, 2381 (1989).
[15] T. S. Hahm and R. M. Kulsrud, Phys. Fluids **28**, 2412 (1985).
[16] T. C. Hender and R. Fitzpatrick, in *Proceedings of the 17th European Conference on Plasma Physics and Controlled Fusion* (E.P.S., Geneva, 1990), Vol. II, p. 923.
[17] R. D. Gill, A. W. Edwards, and A. Weller, Nucl. Fusion **29**, 821 (1989).
[18] D. J. Campbell (private communication).

This article is copyrighted as indicated in the article. Reuse of AIP content is subject to the terms at: http://scitationnew.aip.org/termsconditions. Downloaded to IP: 128.62.18.33 On: Thu, 12 Mar 2015 15:56:36